

Application of volumetric electrodes to the recovery of silver in sulphuric acid solutions.

I. Mass transfer and electrochemical rate

A. RATEL, G. LACOSTE

Laboratoire de Recherche et développement en Génie Chimique (LA CNRS 192), Institut du Génie Chimique, Chemin de la Loge, 31078 Toulouse, France

Received 7 July 1981

A fixed bed reactor working under diffusion control has been used to deposit silver from acidified aqueous solutions containing silver ions. The theoretical description of the cell leads to three equations for concentration, potential and current density, which are solved by a numerical method. Agreement between the theoretical model and the experimental data is obtained for a limited range of flow velocities and heights of the porous bed. Simple expressions for the electrochemical rate and distribution of potential in the porous electrode as a function of the flow velocity direction have been derived.

Nomenclature	R	universal gas constant = $8.31 \text{ J mol}^{-1} \text{ K}^{-1}$
a, b, c	constants	R_p
a_i	activity of the i species	r_{Ag}
C	molecular concentration of electro-active species (mol m^{-3})	S_p
C_{el}	wall concentration (mol m^{-3})	T
$C(0)$	inlet concentration (mol m^{-3})	t
$C(H)$	outlet concentration (mol m^{-3})	u_i
D	diffusion coefficient ($\text{m}^2 \text{ s}^{-1}$)	v
E	local metal solution potential difference (V)	v_e
E_0	standard potential (V)	x
E_0^*	normal modified potential (V)	γ_{Ag}
F	Faraday's constant ($1F = 96.487 \text{ C mol}^{-1}$)	ϵ
H	thickness of porous bed (m)	σ_m
i	current density at the electrode surface (A m^{-2})	σ_0
$J_m, (J_s)$	current density in the solid matrix (in the solution) (A m^{-2})	σ_s
k	average mass transfer coefficient between flowing solution and electrode surface (m s^{-1})	ϕ_m
N_i	mass flux vector of species i ($\text{mol m}^{-2} \text{ s}^{-1}$)	ϕ_s
n	number of electrons transferred during the electrochemical reaction	∇
		$\nabla \cdot$
		∇^2

1. Introduction

Planar electrodes are often used in the treatment of concentrated metal containing solutions. Industrial effluents, however, are dilute solutions of precious, rare or polluting metallic ions, therefore, small current densities are obtained and it is necessary to increase the electrode surface. The use of porous electrodes is one method of achieving this. The flow through porous electrode (fpe) seems to be well adapted for this application [1–6], giving a wide exchange surface area with a reduced volume and offering the advantages of a dynamic system. However, this type of reactor is not easy to design [6, 7] since it is limited by the overall potential drop (opd) which occurs in the solution and sometimes in the solid phase. In an analysis of such a system it is very important to know the local metal–solution potential difference (lpd) within the reactor to: ensure the specificity of the electrochemical reaction; and fix the electrochemical reaction rate. In electroreduction processes the latter condition ensures the quality of the metallic coating [8]. Various authors have considered several types of kinetics such as limiting diffusion [5–7, 9, 10], diffusion [11] and pure activation [12].

In the case of silver recovery from sulphuric acid solution ($[Ag] < 100$ ppm, 1 N H_2SO_4) the interest in diffusion control has been clearly shown [13].

The work presented in this paper deals with: (a) the determination of the electrochemical rate within the reactor; and (b) the calculation of mass conversion in relation to electric (opd), geometric (particle diameters, height of the bed) and hydrodynamic parameters (flow velocity).

2. Experimental procedures

2.1. Experimental design

Figure 1 represents the schematic flow-sheet of the apparatus used including a cell, a rotameter and a pump. The cathode fixed bed consists of silver-coated glass. The anode, where oxygen evolution occurs, is a platinum grid placed: (a) above the porous bed for a cathode \rightarrow anode flow; and (b) under the porous bed for an anode \rightarrow

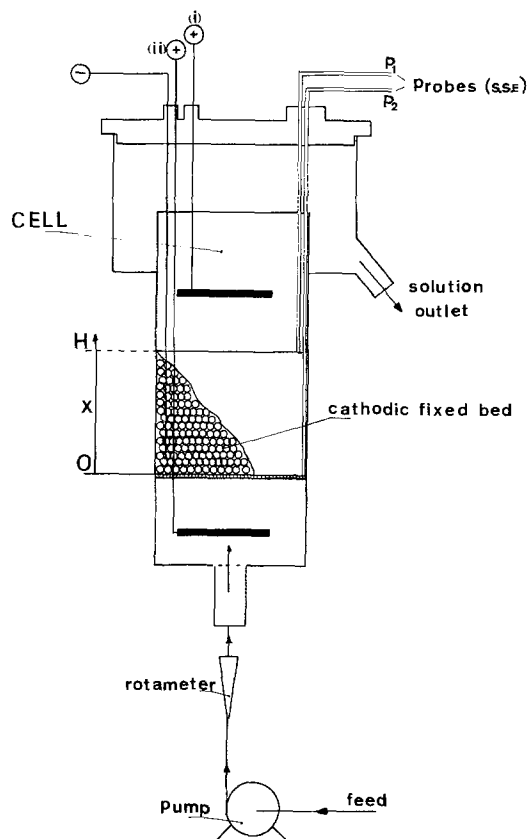


Fig. 1. Flow sheet of the apparatus.

cathode flow. The cross-sectional area of the bed is 13.9 cm^2 . Other parameters considered are the height of the porous bed, H , and the particle diameter, dp . The flow studied crosses the bed with a velocity v_e . The physical and electrochemical properties may be found in Table 1. With a probe, P_1 , in contact with a mercury/saturated potassium sulphate electrode (SSE), the lpd can be fixed for any chosen point in the porous bed. The mobility of P_2 , a probe of

Table 1. Solution characteristics

Physical characteristics at 20° C

Fluid density	$\rho = 1030 \text{ kg m}^{-3}$
Kinematic viscosity	$\nu = 10.5 \times 10^{-7} \text{ m}^2 \text{ s}^{-1}$
Diffusion coefficient	$D = 12 \times 10^{-10} \text{ m}^2 \text{ s}^{-1}$
True conductivity	$\sigma_0 = 20 \Omega^{-1} \text{ m}^{-1}$
Apparent conductivity	$\sigma_s = 6 \times 15 \Omega^{-1} \text{ m}^{-1}$
Silver concentration	$\leq 120 \text{ ppm}$

Electrochemical characteristics

$-0.120 \text{ V/SSE} \leq 1 \text{ ppd} \leq -0.075 \text{ V/SSE}$

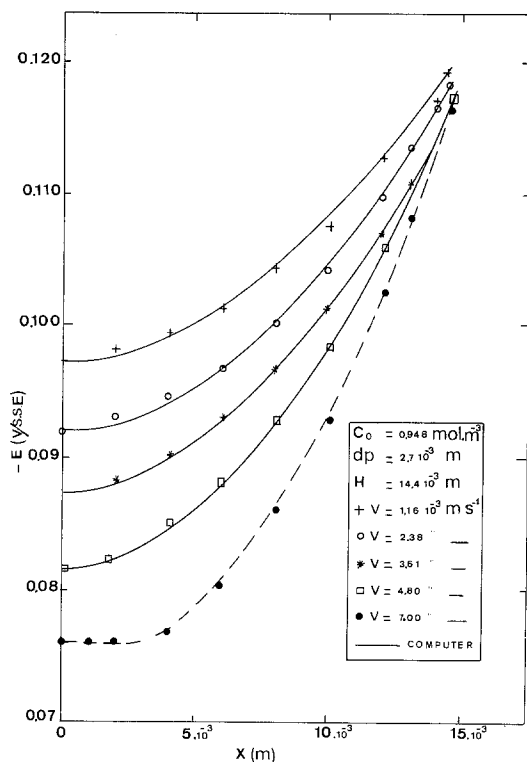


Fig. 2. Distribution of lpd in the porous bed for several flow velocities.

the same type as P_1 , allows the lpd distribution within the cathodic bed to be measured.

2.2. Presentation of the problem

The variation of E with the height of the bed is plotted in Fig. 2. The lpd value increases from

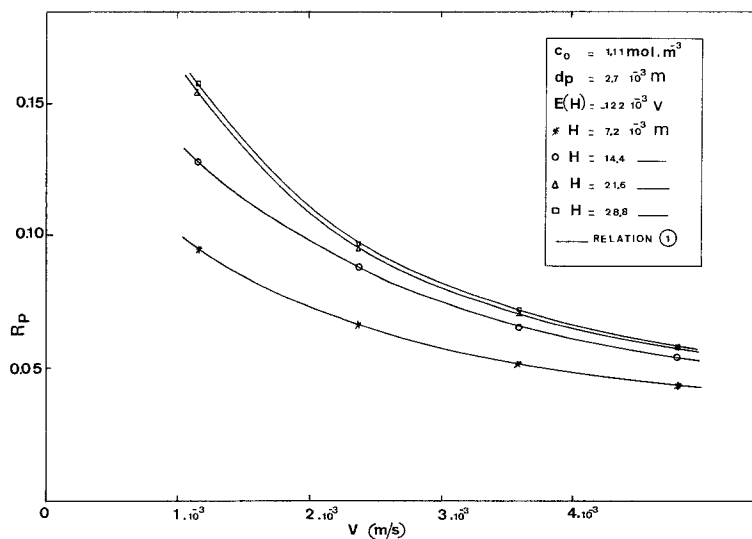


Fig. 3. Variation of reactor yield versus velocity at different heights of the bed.

the top ($x = H$) (where it is fixed at -120 mV vs SSE) to the bottom ($x = 0$). The opd between the top and the bottom of the bed depends on, in particular, the flow velocity, the specific surface area (or particle diameter), the height of the bed and the inlet concentration of silver ions.

This is well known and has been checked with other systems [6] and other electrochemical reactions [12]. In particular, for low x values and for high values of the flow velocity, the lpd is equal to the equilibrium value and, therefore, the electrochemical reaction is not possible. The variation of the yield R_p defined by the relation

$$R_p = \frac{C_{(0)} - C_{(H)}}{C_{(0)}} \quad (1)$$

depends on the flow velocity and is plotted in Fig. 3. The yield decreases as the velocity increases, but when the height of the bed reaches a critical value, the bottom of the bed stays at the equilibrium potential and the yield stops increasing because the working volume of the bed no longer varies with height.

3. Mathematical development

3.1. Transport laws

A material balance for each component, i , under steady-state conditions can be written per unit volume of the solution as

$$\frac{dC_i}{dt} = -\nabla \cdot N_i + r_i = 0. \quad (2)$$

The flux N_i of each chemical species is a vector quantity which depends on migration, diffusion and convection phenomena

$$N_i = -n_i F U_i C_i \nabla \phi_s - D_i \nabla C_i + C_i v_e \quad (3)$$

with the following hypotheses.

For the Ag^+ species, the convective term is much more important than those for diffusion and migration, so the equation of continuity in the liquid phase is:

$$\epsilon \nabla \cdot N_{\text{Ag}^+} = \nabla \cdot (C v_e) = r_{\text{Ag}} \quad (4)$$

but in this case $v_e = v/\epsilon = \text{constant}$, and since the concentration is only a function of the distance x through the porous electrode, Equation 4 becomes:

$$v \cdot \frac{dC_{\text{Ag}^+}}{dx} = r_{\text{Ag}^+} \quad (5)$$

The current in the electrolyte solution is, of course, due to the motion of charged particles (ionic current). The current density vector in the solution phase, J_s , can be expressed by the relation

$$J_s = \sum_i J_i = \sum_i n_i F N_i \quad (6)$$

with Equation 3, and the hypotheses can be simplified if: for all species, i , diffusion due to the concentration gradient is neglected when compared with migration; the solution present in the cathode pores is electrically neutral ($\sum n_i C_i = 0$); and the charge transport in solution is assumed to be essentially due to the H_3O^+ ions (indifferent electrolyte).

Application of Equation 2 allows one to write, for the vector current density in the whole cathode volume,

$$\nabla \cdot J_s = \nabla \cdot J_{\text{Ag}^+} = -\sigma_s \nabla^2 \phi_s \quad (7)$$

where σ_s is the effective conductivity of the solution within the pores, related to the bulk conductivity, σ_0 , as follows [14]:

$$\sigma_s = \sigma_0 \frac{2\epsilon}{3 - \epsilon}$$

Application of Equation 4 yields

$$\nabla \cdot J_s = -\sigma_s \cdot \nabla^2 \phi_s = F r_{\text{Ag}^+} \quad (8)$$

The current variation in the solution is only a

function of the variation in concentration of the electroactive species.

In the metallic matrix, the vector current density (electronic current) J_m follows the global relation

$$\nabla \cdot J_s + \nabla \cdot J_m = 0$$

and so, since J_m follows Ohm's law,

$$\nabla \cdot J_m = -\sigma_m \cdot \nabla^2 \phi_m = F r_{\text{Ag}^+} \quad (9)$$

The lpd value E defined by

$$E = \phi_m - \phi_s$$

follows the relation

$$\nabla^2 E = + \left(\frac{1}{\sigma_m} + \frac{1}{\sigma_s} \right) F r_{\text{Ag}^+}$$

In the present case, the metallic matrix is infinitely conductive ($1/\sigma_m \rightarrow 0$), and the previous relationship gives the general equation of the lpd

$$\nabla E = + \frac{1}{\sigma_s} \cdot J_s \quad (10)$$

Also in this work dealing with the recovery of silver from sulphuric acid solutions using the hypotheses of diffusion control, the electrochemical rate r_{Ag^+} can be expressed by

$$r_{\text{Ag}^+} = -k Sp \left[C - 10^3 \times \exp(E - E_0^*) \frac{F}{RT} \right]$$

The derivation of this expression is explained in the Appendix.

3.2. Solution of the equations

Equations 5, 8 and 10 form a system of differential equations. With their solution, one can obtain the distribution of concentration, C , current density vector, J_s , and lpd within the volumetric electrode.

The analytical solution of such a system is difficult to obtain because of the coupling of concentration and potential.

In this work we have developed a numerical method for solving these equations (Runge-Kutta of fourth-order). The results are plotted in Fig. 4 [$E(x) = f(x)$], Fig. 5 [$C(x) = f(x)$] and Fig. 6 [$r(x) = f(x)$] for the two possible directions of flow (cathode towards anode and the reverse).

The boundary conditions for Equations 5, 8

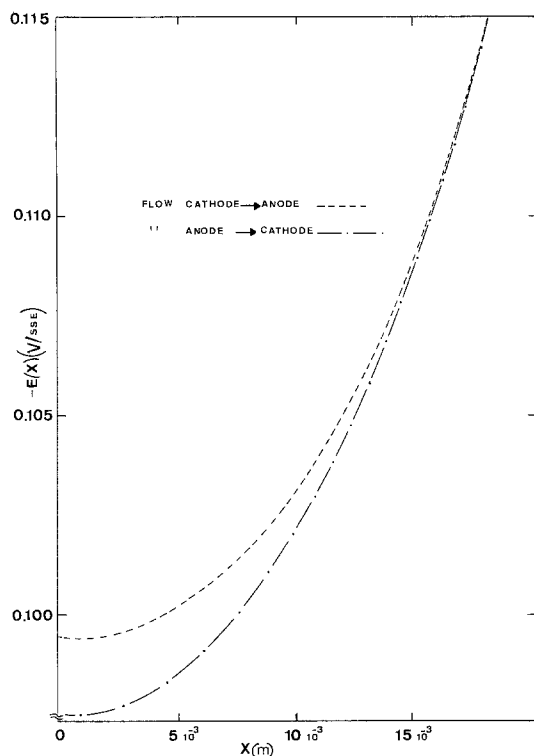


Fig. 4. Variation of $E(x) = f(x)$, for two types of percolation.

and 10 are:

For cathode \rightarrow anode flow

$$C = C_0 \quad \text{at} \quad x = 0$$

$$J_s = 0 \quad \text{at} \quad x = 0$$

$$E(H) = \text{constant} \quad \text{at} \quad x = H$$

For anode \rightarrow cathode flow

$$C = C_0 \quad \text{at} \quad x = 0$$

$$J_s = 0 \quad \text{at} \quad x = H$$

$$E(0) = \text{constant} \quad \text{at} \quad x = 0.$$

4. Results and discussion

It is not easy to check experimentally the current distribution $J_s(x)$ and concentration distribution $C(x)$ within the porous bed, but it is not so difficult to measure the potential in the solution and, therefore, the lpd everywhere in the bed by means of a movable probe. Before giving any interpretation of these results it is convenient to

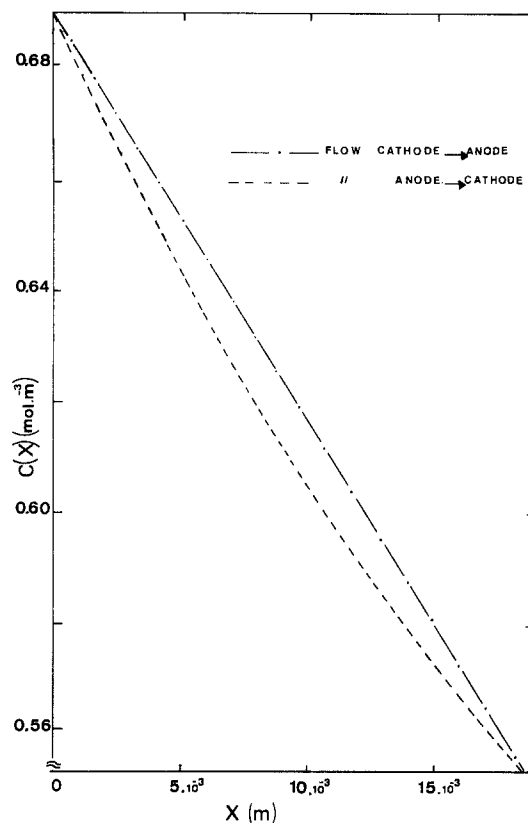


Fig. 5. Variation of $C(x) = f(x)$, for two types of percolation.

look carefully at Fig. 5. For the direction of flow, cathode \rightarrow anode, the variation of concentration $C(x)$ is quite linear. Moreover, Fig. 6 shows that under the same conditions, $r(x)$ is fairly constant all along the reactor. It could be considered to be a differential reactor, the mass balance of which is precisely Equation 5. The presence of a constant kinetic term for a percolating cathode \rightarrow anode is the result of two complementary phenomena: on the one hand, $C(x)$ decreases from $x = 0$ to $x = H$ in a monotonic, quasi-linear way; and on the other hand, the lpd increases (in absolute value) in the same direction. Therefore, the kinetic term appears to be constant for every position, which means that $C(x)$ (cf. Equation 5) has a quasi-linear distribution and that $E(x)$ has the following expression:

$$E(x) = ax^2 + bx + c$$

The three constants a , b and c depend upon the boundary conditions and finally

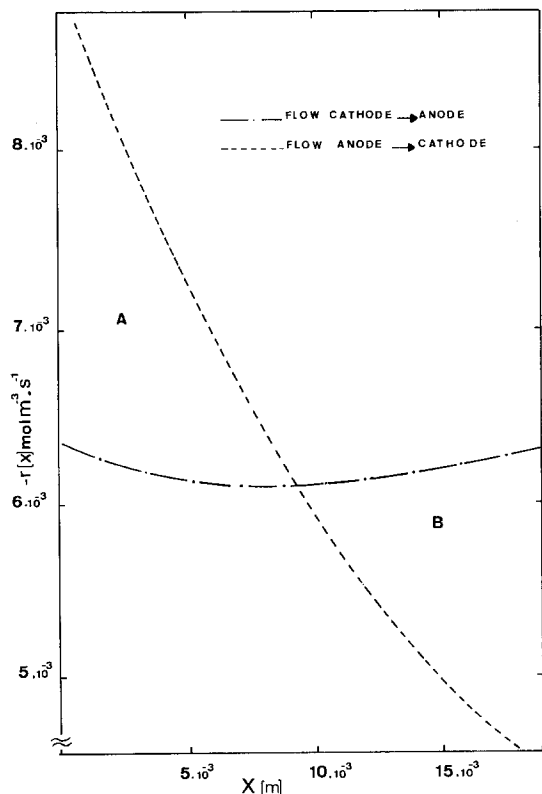


Fig. 6. Variation of $r(x) = f(x)$, for two types of percolation.

$$E(x) - E(H) = -\frac{kFSp}{2\sigma_s} \left(C(0) - 10^3 \right) \times \exp \left\{ [E(0) - E_0^*] \frac{F}{RT} \right\} (x^2 - H^2). \tag{12}$$

Figures 7 and 8 show the variations of $E(x)$

with x^2 for different values of percolation velocity and electrode height.

As indicated before, checking the variation of concentration within the porous bed is not easy. But it is not so difficult to measure the inlet and outlet concentrations. It has been possible to calculate the conversion rate, R_p , both experimentally and theoretically using the expression:

$$R_p = \frac{C(0) - C(H)}{C(0)} = \frac{kSpH}{vC(0)} \times \left(C(0) - 10^3 \times \exp \left[[E(0) - E_0^*] \frac{F}{RT} \right] \right) \tag{13}$$

Figure 9 shows good agreement between these results. The main conclusion is that the yield is quite independent of the direction of percolation (cf. Fig. 5). Moreover, from Fig. 6 one can see that the yield, which was defined as

$$R_p = \frac{1}{vc(0)_0} \int_0^H r(x) dx,$$

is independent of the direction of flow. (The two areas A and B are nearly equal in Fig. 6).

It is necessary to add several comments concerning the overall potential drop, specific to this kind of reactor. The direction of percolation has only a small influence (mean difference of 8%), however, a smaller potential drop was observed in the case of a cathode \rightarrow anode flow.

5. Conclusions

In this first study, we have considered the design of a reactor with a volumetric electrode under

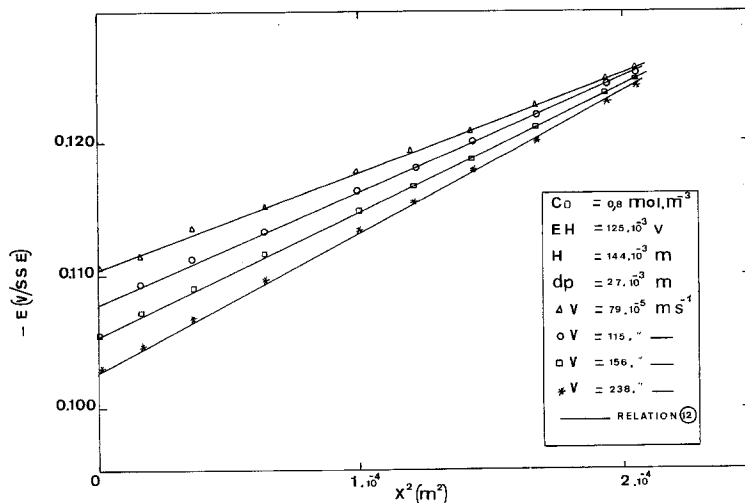


Fig. 7. $E(x) = f(x^2)$ for several flow velocities.

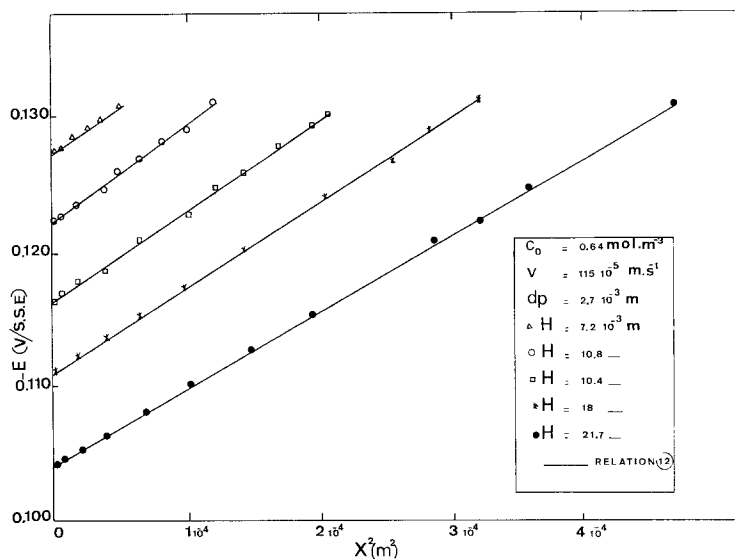


Fig. 8. $E(x) = f(x^2)$ for several heights of the bed.

diffusion control. We have developed differential equations for the calculation of the conversion rate while knowing the opd in relation to the hydrodynamic and electric parameters.

The specific treatment of industrial effluents compels one to work quite often in a narrow range

of metal-solution potential. We have shown here that although the conversion rate remains low, the reactor works with a nearly constant reaction rate throughout the whole volume. This is a desirable operating feature since the approximately uniform current density leads to an evenly distributed silver deposit of uniform quality.

Appendix

Expression for the electrochemical rate r_{Ag^+}

In an electrochemical reaction two phenomena occur: electron transfer occurs with a rate related to the electrode potential; and the electrolysed species leave by diffusion with a certain rate.

It has been shown that when the chemical reactions are taken into account as well as the transfer [15, 16] for a fast system, the electrode potential is

$$E = E_{0/i} + \frac{RT}{nF} \ln (a_i^+)_{el}$$

with $(a_i^+)_{el}$ = activity of the i species at the electrode, $E_{0/i}$ = standard potential of species i .

In the case of silver present at very low concentrations in a sulphuric acid medium (1 N), we are able to write

$$E = E_{0/Ag} + \frac{RT}{F} \ln \gamma_{Ag} + \frac{RT}{F} \ln [Ag^+]_{el}$$

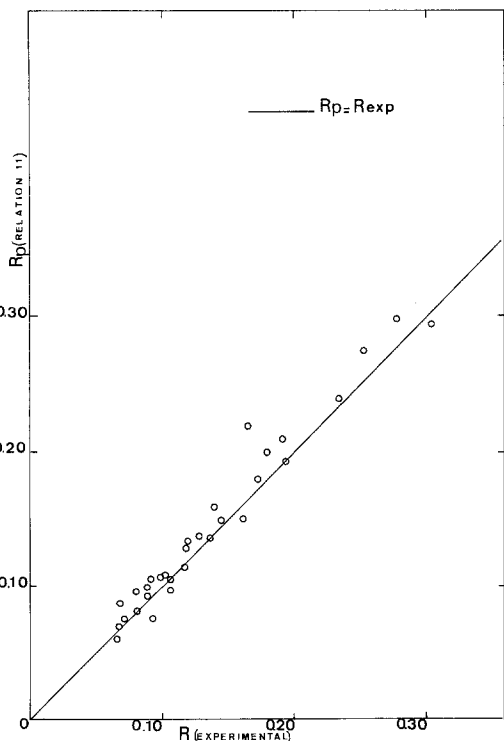


Fig. 9. Comparison between experimental and theoretical yield.

where $E_{0/\text{Ag}} = 0.800 \text{ V}$ and $[\text{Ag}^+]_{\text{el}}$ is the concentration of silver (mol m^{-3}). Furthermore, γ_{Ag} , the activity coefficient of silver, is independent of the silver concentration because of the presence of excess supporting electrolyte.

In this study $\gamma_{\text{Ag}} = 0.040$ and the numerical values of E can be calculated from the expression

$$E = E_0^* + \frac{RT}{F} \ln(10^{-3} \times C_{\text{el}})$$

where C_{el} is the concentration of silver in mol m^{-3} and E_0^* is the normal modified potential of the system. It's expression is:

$$\begin{aligned} E_0^* &= E_{0/\text{Ag}} + \frac{RT}{F} \ln \gamma_{\text{Ag}} \\ &= 0.721 \text{ V} \quad \text{at } 25^\circ \text{ C.} \end{aligned}$$

With respect to the mercury sulphate saturated electrode (SSE), $E_0^* = 0.104 \text{ V}$.

Under steady-state conditions at the electrode surface, the transfer and diffusion kinetics are equal. The local current density, i , is given by

$$i = -Fk [C - C_{\text{el}}]$$

and

$$i = -Fk \left[C - 10^3 \times \exp(E - E_0^*) \frac{F}{RT} \right].$$

Hence, the local reaction term, proportional to the current density, is determined by the expression:

$$r_{\text{Ag}^+} = -kS_p \left[C - 10^3 \times \exp(E - E_0^*) \frac{F}{RT} \right].$$

References

- [1] R. de Levie, 'Advances in Electrochemistry and Electrochemical Engineering', Vol. 6, (edited by P. Delahay) Interscience Publishers, New York (1966).
- [2] R. E. Sioda, *Electrochim. Acta* **16** (1971) 1569.
- [3] D. N. Bennion and J. Newman, *J. Appl. Electrochem.* **2** (1972) 113.
- [4] R. E. Sioda, *Electrochim. Acta* **20** (1975) 457.
- [5] R. Alkire and B. Gracon, *J. Electrochim. Soc.* **122** (1975) 1594.
- [6] F. Coeuret, *Electrochim. Acta* **21** (1976) 203.
- [7] H. Olive and G. Lacoste, *Electrochim. Acta* **25** (1980) 1303.
- [8] J. Amblard and M. Froment, *Surface Technology* **6** (1978) 409.
- [9] J. Newman and W. Tiedeman, *AIChEJ.* **21** (1975) 25.
- [10] P. W. Appel and J. Newman, *AIChEJ.* **22** (1976) 979.
- [11] M. Paulin, D. Hutin and F. Coeuret, *J. Electrochem. Soc.* **2** (1977) 180.
- [12] F. Coeuret, D. Hutin and A. Gaunamd, *J. Appl. Electrochem.* **6** (1976) 417.
- [13] A. Ratel, Thèse de 3è cycle, I.N.P. Toulouse (1980).
- [14] G. H. Neale and W. K. Nader, *AIChEJ.* **19** (1973) 112.
- [15] G. Charlot *et al.* 'Les réactions Electrochimiques', Masson (1959).
- [16] R. E. Sioda, *J. Electroanal Chem. Interfac. Electrochem.* **34** (1972) 399.